A fast algorithm for the electromagnetic scattering from a large cavity

Bao, Gang; Sun, Weiwei

Published in:
SIAM Journal on Scientific Computing

Published: 01/01/2006

Document Version:
Final Published version, also known as Publisher's PDF, Publisher's Final version or Version of Record

Published version (DOI):
10.1137/S1064827503428539

Publication details:
Bao, G., & Sun, W. (2006). A fast algorithm for the electromagnetic scattering from a large cavity. *SIAM Journal on Scientific Computing*, *27*(2), 553-574. https://doi.org/10.1137/S1064827503428539

SIAM J. SCI. COMPUT.
Vol. 27, No. 2, pp. 553–574

A FAST ALGORITHM FOR THE ELECTROMAGNETIC SCATTERING FROM A LARGE CAVITY*

GANG BAO† AND WEIWEI SUN‡

Abstract. A fast algorithm is presented for solving electromagnetic scattering from a rectangular open cavity embedded in an infinite ground plane. The medium inside the cavity is assumed to be (vertically) layered. By introducing a transparent (artificial) boundary condition, the problem in the open cavity is reduced to a bounded domain problem. A simple finite difference method is then applied to solve the model Helmholtz equation. The fast algorithm is designed for solving the resulting discrete system in terms of the discrete *Fourier transform* in the horizontal direction, a Gaussian elimination in the vertical direction, and a preconditioning conjugate gradient method with a complex diagonal preconditioner for the indefinite interface system. The existence and uniqueness of the finite difference solution are established for arbitrary wave numbers. Our numerical experiments for large numbers of mesh points, up to 16 million unknowns, and for large wave numbers, e.g., between 100 and 200 wavelengths, show that the algorithm is extremely efficient. The cost for calculating the radar cross section, which is of significant interest in practice, is $O(M^2)$ for an $M \times M$ mesh. The proposed algorithm may be extended easily to solve discrete systems from other discretization methods of the model problem.

Key words. electromagnetic scattering, FFT, preconditioning, indefinite systems

AMS subject classifications. 78M20, 65N22, 65N06

DOI. 10.1137/S1064827503428539

1. Introduction.

As a measure of the detectability of a target in radar systems, radar cross section (RCS) has been an important subject of study in electromagnetics. Accurate prediction of the RCS of complex objects such as aircraft presents a great challenge in computational electromagnetics. Of particular importance is the RCS prediction of cavities due to its dominance to the target's overall RCS. Examples of cavities include jet engine inlet ducts, exhaust nozzles, and cavity-backed antennas. The computation is especially challenging when the cavities are large compared to the wavelength of the fields because of the highly oscillatory nature of the fields. This paper is intended to develop a fast algorithm for solving the electromagnetic scattering problem from large cavities. More specifically, consider a time-harmonic electromagnetic plane wave incident on an open cavity embedded in an infinite ground plane. The geometry is shown in Figure 1. The ground plane and the walls of the open cavity are perfect electric conductors (PEC), and the interior of the open cavity is filled with nonmagnetic material which may be inhomogeneous. The half-space above the ground plane is filled with a homogeneous, linear, isotropic medium. In this setting, the electromagnetic scattering by the cavity is governed by the Helmholtz equation along with Sommerfeld's radiation conditions imposed at infinity.

*Received by the editors May 27, 2003; accepted for publication (in revised form) March 15, 2005; published electronically October 31, 2005.
http://www.siam.org/journals/sisc/27-2/42853.html

†Department of Mathematics, Michigan State University, East Lansing, MI 48824-1027 (bao@math.msu.edu) and School of Mathematics, Jilin University, Changchun, China. The research of this author was partially supported by NSF grant DMS 01-04001, ONR grant N000140210365, and NSF of China grant 10428105.

‡Department of Mathematics, City University of Hong Kong, Hong Kong (maweiw@math.cityu.edu.hk). The research of this author was supported in part by a grant from the Research Grants Council of the Hong Kong Special Administrative Region, China (project CityU 1141/01P).

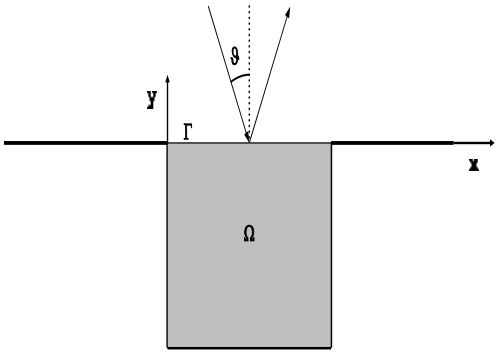

FIG. 1. *The cavity geometry.*

Because of its significant industrial and military applications, the cavity problem has attracted much attention recently. A variety of numerical methods including finite difference, finite element, boundary element methods, and hybrid methods have been developed by the engineering community for solving the open cavity problems [27], [34], [35], [42]. A detailed discussion and additional references may be found in Jin [23]. Mathematical analysis of open cavity models has been conducted by an integral equation method [2], and by a variational approach [3]. An important step for solving the open cavity problem is to introduce a transparent boundary condition on the top line of the cavity. The boundary condition reduces the infinite problem to a finite computational domain, which in turn can be solved by some classical numerical approximation. More recently, a time-domain finite element method has been presented in [41]. However, efficient solvers for the discrete linear systems have not been explored. Classical direct and iterative algorithms are not efficient, especially for large cavity problems due to their high computational costs.

The problem with large wave number, or more precisely with large "ka" number, is of significant interest. Here k is the wave number and a is the diameter of the computational domain. For electromagnetic cavity problems, microwaves are usually considered. Nonetheless, for large cavities, the large domain diameters give rise to high "ka" numbers. Our goal in this paper is to develop a fast algorithm that is capable of dealing with large cavities. For convenience, without loss of generalities, we focus primarily on high wave number problems in our discussion. A straightforward change of coordinates yields the equivalence of high wave number and large cavity problems in the current context. The main difficulty lies in the fact that the solution at a high wave number is highly oscillatory. Moreover, it is well known that error estimates strongly depend upon the wave number. Babuska and Sauter [5] showed that for a related model problem, the ratio of the error of the Galerkin solution and the error of the best approximation tends to infinity as the wave number increases. Furthermore, Aziz, Kellogg, and Stephen [4] pointed out that the condition "k^2h small" would be required to guarantee that the error of the Galerkin solution has the same magnitude as the error of the best approximation, where h is the mesh size. For a large cavity problem, say $1m \times 1m$, with a centimeter incident wave, this condition implies that $h \approx 10^{-4}m$, or 10^8 unknowns in the discrete linear systems of two-dimensional cases.

In this paper, we present a fast algorithm for solving the electromagnetic scattering from a rectangular cavity in which the medium is y-directional inhomogeneous. The algorithm is based on the use of discrete *Fourier transform* in the horizontal

direction and a Gaussian elimination in the vertical direction. We reduce the global system with an $M \times M$ mesh to a (interface) linear system on the top line of the cavity by $O(M^2)$ operations. Since the interface system is complex and indefinite, i.e., its eigenvalues are located on both sides of the y-axis, many classical iterative methods may not be convergent. Here, we propose a complex diagonal preconditioner for the interface system. All eigenvalues of the preconditioned coefficient matrix lie on the right side of the y-axis and the condition number of the matrix increases slightly as the number of mesh points increase. The BiCG method with the diagonal preconditioner is applied to solve the interface system. The number of iterations used in the BiCG method is almost independent of the number of mesh points. Numerical experiments for large numbers of mesh points, up to 16 million unknowns, and for large wave number, e.g., k is between 100 and 200 wavelengths, show that the algorithm is efficient and the computational cost for RCS is $O(M^2)$ for an $M \times M$ mesh. The existence and uniqueness for discrete system with general approximations to the nonlocal boundary condition are established. Here a simple finite difference method is employed for the approximation to illustrate the idea for solving the scattering problem. It should be pointed out that the proposed algorithm and corresponding analysis may also be extended to linear systems resulting from other discrete approximations.

A related topic is the so-called *fast Poisson's solvers*, which were well studied in the last several decades; see the review papers [39], [40] for finite difference methods and [7], [36], [38] for other approximations. These methods can be applied mainly for solving Poisson's equation on a rectangular region with simple local boundary conditions, such as Dirichlet, Neumann, or periodic boundary conditions. The computational complexity is $O(N^2 logN)$ for an $N \times N$ mesh. Extensions to regions with rectangular substructures and to more general regions can be done in terms of domain decomposition or capacitance matrix techniques [8], [9], [33], [11].

Extensions of capacitance matrix methods to the Helmholtz equations were studied in [16], [17], [30]. For capacitance matrix methods, one needs to solve a capacitance system of small size by using either a direct method with an explicit formula of capacitance matrix or an iterative method in implicit form. At each iteration of the iterative method, the multiplication of a vector by the capacitance matrix can be performed by the classical fast Poisson solver. Usually, direct methods for solving capacitance systems are more expensive [33].

There are two related Helmholtz type models: exterior and interior Helmholtz problems. The former concerns the scattering from a bounded medium or obstacle; while the latter deals with the Helmholtz equation in a bounded domain with suitable boundary conditions, such as of Dirichlet, Neumann, or impedance (Robin) types. Numerous studies have been devoted to the development of iterative algorithms for solving large scale linear systems arising from these two Helmholtz models [12], [13], [14], [16], [17], [18], [21], [26], [31]. The methods are mostly based on domain decomposition and preconditioning techniques. Ernst and Golub [18] solved the interior Helmholtz model in a rectangular domain with impedance boundary conditions using preconditioning methods. In particular, they proposed several preconditioners including the discrete Helmholtz operators with Dirichlet or Neumann boundary conditions on two edges and a preconditioned Schur complement. Elman and O'Leary [12] further studied the first preconditioner proposed in [18] and presented eigenvalue analysis for the preconditioned systems. For the one-dimensional model, the identification of the eigenvalues of a preconditioned system entails the computation of the eigenvalues for a 2×2 matrix. They also extended the algorithm to three-dimensional models with large wavenumbers. More numerical experiments were given in [13].

Note that at each preconditioning iteration of their algorithm, one needs to solve the Helmholtz equation with Dirichlet or Neumann boundary conditions on two edges and impedance boundary conditions on the other two edges, which can be performed by classical FFT-type fast solver.

Exterior Helmholtz problems, in terms of some transformations or truncation techniques, can be reduced to finite domain problems with certain nonlocal boundary conditions: exact, approximate, periodic and Fourier-type, which have been done in the last 30 years; e.g., see [15], [19], [25]. Computational methods for exterior Helmholtz problems with some nonlocal boundary conditions were studied in [16], [17], [20], [28], [31]. In [16], [17], Ernst proposed a fast capacitance matrix algorithm for the exterior Helmholtz equation. A transparent (exact nonlocal) boundary condition introduced in [25] was applied on a circular artificial boundary. Due to the nature of axial symmetry, the nonlocal operator is circulant (periodic). A Krylov subspace method may be used for solving the resulting capacitance system. The multiplication of a vector by the capacitance matrix was performed using a fast Helmholtz solver in an annular domain, which should be viewed as a direct application of fast Poisson's solver since the nonlocal boundary condition is periodic. Otto and Larsson [31] presented a preconditioning algorithm for solving a Helmholtz problem in a duct with a curved bottom, in which a fast Helmholtz solver for a duct with straight lines was used as a preconditioner. The nonlocal boundary conditions at the near- and far-zone boundaries were given in the form of the coupled mode solution. The Fourier-sine transform was applied on both the Helmholtz equation and the nonlocal boundary condition. However, the coupled mode boundary condition proposed in [19] and [1] is only valid for waveguide models rather than the underlying cavity models. The algorithm proposed in the current paper is also based on FFT-type fast solvers and efficient preconditioning techniques. We focus on the cavity model which is different from both the exterior and interior Helmholtz problems. The nonlocal boundary operator arising from the cavity model is not circulant, and the coupled mode boundary condition is not suitable in this case.

Note that efficient numerical algorithms for solving linear systems arising from large cavity models have not been explored. Mathematical analysis on existence and uniqueness of solutions has been conducted only recently in [2], [3]. In our algorithm, the FFT-sine transform with a Gaussian elimination is used to reduce the global system to an aperture system. This step is equivalent to determining the discrete Dirichlet-to-Neumann map. The simple diagonal complex preconditioner applied to the resulting aperture system depends upon both the Helmholtz operator and the nonlocal boundary condition on the aperture. In comparison, the cost at each iteration of our algorithm is proportional to $NlogN$ for an $N \times N$ mesh while the cost at each iteration in [12], [13], [16], [17] is $O(N^2 logN)$.

The rest of the paper is organized as follows. In section 2, the model scattering problem is formulated and further reduced to a bounded domain problem. A detailed fast algorithm is introduced in section 3 for the TM (transverse magnetic) case. Issues on implementation and complexity of the algorithm are addressed. A complex diagonal preconditioner is proposed and the TE (transverse electric) case is also studied. The existence and uniqueness of the finite difference solution is proved in section 4. Section 5 is devoted to numerical experiments of the algorithm. The paper is concluded in section 5 by some general remarks on the usefulness of the algorithm and future directions.

2. The electromagnetic cavity problem. We focus on a two-dimensional geometry by assuming that the medium and material are invariant in the z-direction.

Assume also that the medium is nonmagnetic and a constant magnetic permeability $\mu = \mu_0$ exists everywhere. The electromagnetic property of the medium is characterized by the dielectric coefficient ε. Throughout, it is assumed that ε is layered inside the cavity.

For the TM polarization, in which the magnetic field is transverse to the invariant direction and $E = (0, 0, u(x, y))$, the time-harmonic Maxwell equations reduce to

$$\begin{aligned} &\Delta u + k^2 u = f(x,y) && (x,y) \in \Omega \cup R_2^+, \\ &u = 0 && \text{on } \partial(\Omega \cup R_2^+) \end{aligned} \tag{2.1}$$

together with the radiation boundary condition

$$\lim_{r\to\infty} r\left(\frac{\partial u}{\partial \eta} - ik_0 u\right) = 0, \tag{2.2}$$

where $k^2 = \omega^2 \varepsilon \mu_0$ and R_2^+ denotes the upper half-space. Inside Ω, assume that $\varepsilon = \varepsilon(y)$ is independent of the variable x. The fields are said to be source free if the source term $f = 0$.

For the TE polarization, in which the electric field is transverse to the invariant direction, $H = (0, 0, u(x, y))$, the Maxwell equations reduce to

$$\begin{aligned} &\nabla \cdot \left(\frac{1}{k^2}\nabla u\right) + u = f(x,y) && (x,y) \in \Omega \cup R_2^+, \\ &\frac{\partial u}{\partial n} = 0 && \text{on } \partial\Omega \setminus \Gamma \end{aligned} \tag{2.3}$$

with the same radiation boundary condition (2.2). Here, n denotes the unit outward normal.

Since the upper half-space is homogeneous, a so-called transparent boundary condition can be obtained by using either Green's function method (i.e., Hankel's function) [23] or the method of Fourier's transform [2], [3], [15]. In the TM case, the scattering problem may be further reduced to a bounded domain problem:

$$\begin{aligned} &\Delta u + k^2 u = f(x,y) && (x,y) \in \Omega, \\ &u = 0 && \text{on } \partial\Omega \setminus \Gamma, \\ &\frac{\partial u}{\partial n} = I(u) && \text{on } \Gamma, \end{aligned} \tag{2.4}$$

where $I(u)$ denotes a nonlocal integral operator on Γ.

Let $G_d(\boldsymbol{x}, \boldsymbol{x}')$ be the upper half-plane Dirichlet Green's function for the Helmholtz equation

$$G_d(\boldsymbol{x}, \boldsymbol{x}') = \frac{\mathrm{i}}{4}\left[H_0^{(1)}(k\boldsymbol{r}) - H_0^{(1)}(k\bar{\boldsymbol{r}})\right], \tag{2.5}$$

where $\boldsymbol{x} = (x, y)$, $\boldsymbol{x}' = (x', y')$, $\boldsymbol{r} = |\boldsymbol{x} - \boldsymbol{x}'|$, $\bar{\boldsymbol{r}} = |\boldsymbol{x} - \bar{\boldsymbol{x}}'|$ and $\bar{\boldsymbol{x}}' = (x', -y')$ is the image of $\boldsymbol{x}$ with respect to real axis; by Green's theorem and noting the homogeneous boundary conditions,

$$u(x,y) = \int_\Gamma \frac{\partial G_d(x, y; x', 0)}{\partial n'} u(x')dx' \quad x \in (0, a). \tag{2.6}$$

Then the nonlocal boundary condition is given by

$$\frac{\partial u}{\partial y} = I(u) := -\frac{\mathrm{i}k_0}{2} \text{⨍}_\Gamma \frac{1}{|x-x'|} H_1^{(1)}(k_0|x-x'|)u(x')dx' \quad x \in (0,a), \tag{2.7}$$

where ⨍_Γ denotes a Hadamard principle value (or finite part) integral. An alternative Fourier-type nonlocal boundary condition given in [1] is

$$I(u) = \frac{\mathrm{i}k_0}{2} \int_R \sqrt{k_0^2 - \xi^2}\mathcal{F}[\tilde{u}]e^{\mathrm{i}\xi x}d\xi,$$

where $\tilde{u}$ is an extension of u to $H^{1/2}(R)$ and $\mathcal{F}$ denotes the Fourier transformation.

Similar nonlocal boundary conditions for other geometries may be found in [15] and [19].

Assume that a plane wave $u_I = e^{\mathrm{i}(\alpha x - \beta y)}$ is incident on the cavity from the above, where $\alpha = k_0 \sin\theta$, $\beta = k_0 \cos\theta$, and $-\pi/2 < \theta < \pi/2$ is the angle of incidence with respect to the positive y-axis. The scattered field u^s can be expressed by

$$u^s = u^t - u_I + e^{\mathrm{i}(\alpha x + \beta y)},$$

where u^t is the total field of the scattering problem. Since u^s satisfies the Helmholtz equation (2.1) and the radiation condition (2.2), the total field u^t satisfies the following equation:

$$\begin{aligned} &\Delta u + k^2 u = f(x,y) && (x,y) \in \Omega, \\ &u = 0 && \text{on } \partial\Omega \setminus \Gamma, \\ &\frac{\partial u}{\partial n} = I(u) + g(x) && \text{on } \Gamma, \end{aligned} \tag{2.8}$$

where $g(x) = 2\mathrm{i}\beta e^{\mathrm{i}\alpha x}$.

Similarly, one can derive the formulation for TE polarization. In this case, the corresponding Helmholtz-type equation and the transparent boundary condition for the total field are

$$\begin{aligned} &\nabla \cdot \left(\frac{1}{k^2}\nabla u\right) + u = f(x,y) && (x,y) \in \Omega, \\ &\frac{\partial u}{\partial n} = 0 && \text{on } \partial\Omega \setminus \Gamma, \\ &\frac{\partial u}{\partial n} = \tilde{I}(u) + g && \text{on } \Gamma, \end{aligned} \tag{2.9}$$

where $\tilde{I}(u)$ is a nonlocal integral operator.

The existence and uniqueness of solutions of (2.8) and (2.9) for arbitrary wave numbers have been obtained in [3]. The proof is based on a variational approach by using the Fredholm alternative along with the fact that the imaginary part of the nonlocal integral operator is nonnegative.

When a numerical approximation is used for the discretization of (2.8), the global system can be written in general by

$$\begin{pmatrix} A & A_{12} \\ A_{21} & B \end{pmatrix} \begin{pmatrix} u \\ u_B \end{pmatrix} = \begin{pmatrix} f \\ g \end{pmatrix}, \tag{2.10}$$

where A denotes the discrete Helmholtz operator and B corresponds to the discrete boundary integral operator. The matrix A is sparse and B is full in general. Direct methods for such a system are generally less efficient. Most numerical algorithms are based on a Schur complement technique [23], [32]. A particular one is the outward-looking approach, i.e.,

$$\begin{aligned} &(A - A_{12}B^{-1}A_{21})u = f - A_{12}B^{-1}g, \\ &Bu_B = g - A_{21}u\,. \end{aligned} \tag{2.11}$$

Alternatively, there is also the inward-looking approach

$$\begin{aligned} &(B - A_{21}A^{-1}A_{12})u_B = g - A_{21}A^{-1}g, \\ &Au = f - A_{12}u_B. \end{aligned} \tag{2.12}$$

Some classical iterative algorithms, such as conjugate gradient and biconjugate gradient methods, have been applied for solving these subsystems or directly for solving the global system (2.10). The computational cost at each iteration in (2.11) or (2.12) is at least $O(M^2)$ or $O(M^2 log M)$, respectively. The main purpose of this paper is to present a fast algorithm for solving the Helmholtz equations (2.8) and (2.9) with the nonlocal boundary conditions. Due to the fixed position of aperture in this cavity model, approximate local boundary conditions are not suitable [15]. Also we point out that no convergence result for these iterative methods, particularly for problems with large wave numbers, is available at present.

3. Fast algorithm. For simplicity, we consider a simple five-point finite difference method for the discretization of the Helmholtz equation with uniform meshes and assume that the wave number k is real and positive. The approach may be extended easily to many other approximations. Also, for the layered medium problems in TE polarization, nonuniform meshes in y-direction and some special treatment on interface may be used to achieve better accuracy.

3.1. Algorithm in the TM case. Let $\{x_i, y_j\}_{i,j=0}^{M+1,N+1}$ define a uniform partition of $\Omega = [0, a] \times [-b, 0]$ with $x_{i+1} - x_i = h_x$ and $y_{j+1} - y_j = h_y$. Let v_{ij} be the finite difference solution at the point (x_i, y_j). The discrete finite difference system in the TM case can be given by

$$\frac{v_{i-1,j} - 2v_{ij} + v_{i+1,j}}{h_x^2} + \frac{v_{i,j-1} - 2v_{ij} + v_{i,j+1}}{h_y^2} + \omega\varepsilon(y_j)\mu_0 v_{ij} = f(x_i, y_j),$$
$$i = 1, 2, \ldots, M; j = 1, 2, \ldots, N$$

or in matrix form,

$$(A_x \otimes I_N + I_M \otimes A_y + I_M \otimes D)\, v + (I_M \otimes a_{N+1})\, v_{N+1} = f, \tag{3.1}$$

where $\otimes$ denotes the tensor product (Kronecker product), I_M is the $M \times M$ identity matrix,

$$A_x = \frac{1}{h_x^2}\begin{pmatrix} -2 & 1 & & \\ 1 & -2 & 1 & \\ & \ddots & \ddots & \ddots \\ & & 1 & -2 \end{pmatrix} \qquad A_y = \frac{1}{h_y^2}\begin{pmatrix} -2 & 1 & & \\ 1 & -2 & 1 & \\ & \ddots & \ddots & \ddots \\ & & 1 & -2 \end{pmatrix}$$

$$D = w^2\mu_0 \begin{pmatrix} \varepsilon(y_1) & & & \\ & \varepsilon(y_2) & & \\ & & \ddots & \\ & & & \varepsilon_(y_N) \end{pmatrix} \qquad a_{N+1} = \frac{1}{h_y^2} \begin{pmatrix} 0 \\ \vdots \\ 0 \\ 1 \end{pmatrix}$$

and

$$v = (v_{11}, \ldots, v_{1N}, v_{21}, \ldots, v_{2N}, \ldots, v_{M1}, \ldots, v_{MN})^T,$$
$$v_j = (v_{1j}, v_{2j}, \ldots, v_{Mj})^T.$$

By using a backward finite difference scheme and a general approach for the nonlocal boundary condition, we obtain

$$\frac{v_{i,N+1} - v_{i,N}}{h_y} = \sum_{l=1}^{M} g_{il} v_{l,N+1} + g(x_i), \quad i = 1, 2, \ldots, M,$$

i.e.,

$$-v_N + (I_M - h_y G) v_{N+1} = h_y g,$$

where $G = (g_{ij})_{i,j=1}^M$ is an $M \times M$ matrix.

The global system is given by

$$\begin{pmatrix} A & A_{12} \\ A_{21} & I_M - h_y G \end{pmatrix} \begin{pmatrix} v \\ v_{N+1} \end{pmatrix} = \begin{pmatrix} f \\ h_y g \end{pmatrix}, \tag{3.2}$$

where

$$A = A_x \otimes I_N + I_M \otimes A_y + I_M \otimes D,$$
$$A_{12} = I_M \otimes a_{N+1},$$
$$A_{21} = -h_y^2 A_{12}^T.$$

For the tridiagonal Toeplitz matrix A_x, we have

$$S_M A_x S_M = \Lambda = \begin{pmatrix} \lambda_1 & & & \\ & \lambda_2 & & \\ & & \ddots & \\ & & & \lambda_M \end{pmatrix},$$

where S_M denotes the discrete Fourier-sine transformation,

$$S_M = \frac{1}{\sqrt{M}} \left(\sin \frac{lm\pi}{M+1} \right)_{l,m=1}^{M}, \qquad \lambda_l = -\frac{4(M+1)^2}{a^2} \sin^2 \frac{l\pi}{2(M+1)},$$

and $S_M^2 = I$.

By the discrete Fourier-sine transformation, we rewrite the discrete Helmholtz system (3.1) as

$$(\Lambda \otimes I_N + I_M \otimes A_y + I_M \otimes D)\, \bar{v} + (I_M \otimes a_{N+1})\, \bar{v}_{N+1} = \bar{f}, \tag{3.3}$$

where

$$\bar{v} = (S_M \otimes I_N)\, v = (\bar{v}_{11}, \ldots, \bar{v}_{1N}, \bar{v}_{21}, \ldots, \bar{v}_{2N}, \ldots, \bar{v}_{M1}, \ldots, \bar{v}_{MN})^T, \quad \bar{v}_{N+1} = S_M v_{N+1},$$
$$\bar{f} = (S_M \otimes I_N)\, f = (\bar{f}_{11}, \ldots, \bar{f}_{1N}, \bar{f}_{21}, \ldots, \bar{f}_{2N}, \ldots, \bar{f}_{M1}, \ldots, \bar{f}_{MN})^T.$$

Similarly, the discrete boundary equations become

$$-\bar{v}_N + S_M(I_M - h_y G)S_M\bar{v}_{N+1} = \bar{g},$$

where $\bar{g} = h_y S_M g$.

Reordering the unknowns and equations in (3.3), we obtain

$$\begin{aligned} &(A_y + \lambda_i I_N + D)\hat{v}_i + a_{N+1}\bar{v}_{i,N+1} = \hat{f}_i, \qquad i = 1, 2, \ldots, M, \\ &-\bar{v}_N + S_M(I_M - h_y G)S_M\bar{v}_{N+1} = \bar{g}, \end{aligned} \tag{3.4}$$

where

$$\begin{aligned} &\hat{v}_i = (\bar{v}_{i1}, \bar{v}_{i2}, \ldots, \bar{v}_{iN}), \\ &\hat{f}_i = (\bar{f}_{i1}, \bar{f}_{i2}, \ldots, \bar{f}_{iN}), \qquad i = 1, 2, \ldots, M. \end{aligned}$$

We use the Gaussian elimination method with a row partial pivoting to solve the first system in (3.4). Let

$$A_y + \lambda_i I_N + D = L_i U_i, \quad i = 1, 2, \ldots, M$$

be the LU-decomposition, where $A_y + \lambda_i I_N + D$ is a symmetric tridiagonal matrix.

Since L_i is nonsingular,

$$U_i\bar{v}_i + L_i^{-1}a_{N+1}\bar{v}_{i,N+1} = \hat{f}_i, \qquad i = 1, 2, \ldots, M, \tag{3.5}$$

where $U_i = (r_{pq}^i)$ and $\hat{f}_i = L_i^{-1}\bar{f}_l$.

Combining the last equations of the systems (3.5) and the boundary equations gives

$$\begin{aligned} &r_{NN}^i\bar{v}_{iN} + r_{N,N+1}^i\bar{v}_{i,N+1} = \hat{f}_{iN}, \quad i = 1, 2, \ldots, M, \\ &-\bar{v}_N + S_M(I_M - h_y G)S_M\bar{v}_{N+1} = \bar{g}, \end{aligned} \tag{3.6}$$

where $r_{N,N+1}^i$ is the last component of $L_i^{-1}a_{N+1}$.

Since

$$\begin{aligned} &\bar{v}_N = (\bar{v}_{1N}, \bar{v}_{2N}, \ldots, \bar{v}_{MN}), \\ &\bar{v}_{N+1} = (\bar{v}_{1,N+1}, \bar{v}_{2,N+1}, \ldots, \bar{v}_{M,N+1}), \end{aligned}$$

only $\bar{v}_N$ and $\bar{v}_{N+1}$ are involved in the system (3.6).

If k^2 is not an eigenvalue of the Helmholtz operator with Dirichlet boundary conditions, then for h small enough,

$$r_{NN}^i \neq 0, \qquad i = 1, 2, \ldots, M. \tag{3.7}$$

We can further eliminate the vector $\bar{v}_N$ from the second system in (3.6) to get

$$(S_M(I_M - h_y G)S_M + E)\bar{v}_{N+1} = \hat{g} \tag{3.8}$$

or equivalently

$$(I_M - h_y G + S_M E S_M)v_{N+1} = S_M\hat{g},$$

where

$$E = \begin{pmatrix} r_{1,N+1}^1/r_{NN}^1 & & \\ & \ddots & \\ & & r_{N,N+1}^M/r_{NN}^M \end{pmatrix}$$

and

$$\hat{g}_i = \bar{g}_i + \bar{f}_{iN}/r^i_{NN}, \quad i = 1, 2, \ldots, M.$$

Solving the linear system (3.8) gives the solution v_{N+1} on the interface Γ. The rest of the unknowns can be obtained by solving the following system:

$$(A_y + \lambda_i I_N + D)\bar{v}_i = -a_{N+1}\bar{v}_{N+1}, \quad i = 1, 2, \ldots, M, \tag{3.9}$$

in which $\bar{v}_N = -\bar{g} + \bar{B}\bar{v}_{N+1}$ may be used for those possible nearly singular systems.

If k^2 (approximately) is an eigenvalue of the Dirichlet–Helmholtz operator, then the matrix $A_y + \lambda_i I_N + D$ is singular (or nearly singular) for some $i \in J_s$, where J_s is a subset of $\{1, 2, \ldots, M\}$. Combining the equations in the first system of (3.6) with $i \in J_s$ and a system corresponding to (3.5), we have

$$\begin{bmatrix} D_s & W_{12} \\ W_{21} & I_M - h_y G + S_M E S_M \end{bmatrix} \begin{bmatrix} w \\ v_{N+1} \end{bmatrix} = \begin{bmatrix} f_s \\ g_s \end{bmatrix}, \tag{3.10}$$

where D_s is a diagonal matrix whose diagonal entries consist of r^i_{NN} with $i \in J_s$ and f_s and g_s can be defined analogously. It is obvious that for those i's satisfying

$$\frac{4(N+1)^2}{b^2}\sin^2\frac{\pi}{2(N+1)} + \frac{4(M+1)^2}{a^2}\sin^2\frac{i\pi}{2(M+1)} > k^2.$$

$A_y + \lambda_i I_N + D$ is symmetric negative definite. In all of our numerical tests, J_s is empty, i.e., it suffices to solve the system (3.8).

The algorithm is given below.

Algorithm I

(i) Generate the matrix G.
(ii) Calculate the LU decomposition to get U_i and E by using the forward Gaussian elimination with a row partial pivoting.
(iii) Calculate $\bar{f} = (S_M \otimes I)f$ and $S_M\hat{g}$.
(iv) Solve the system (3.8) for v_{N+1}.
(v) Solve the system (3.9) for the rest of the unknowns.

3.2. Implementation and preconditioning. It should be noted that the nonlocal integral operator is a symmetric Toeplitz-type operator. A suitable approximation to the nonlocal integral operator gives the symmetric Toeplitz matrix G and hence only M entries need be calculated. The nonlocal integral operator is hypersingular. Numerical calculation for such hypersingular integrals has been well studied; e.g., see [37]. Usually, the Hankel function can be evaluated in terms of its series representations or integral representations. One can use some high-order approximation to the Hankel function; hence the cost of Step (i) is $O(M^{1+\sigma})$, where $0 < \sigma < 1$. In Step (ii), one needs to calculate the LU-decomposition for $A_y + \lambda_i I_N + D$. By noting the tridiagonal structure of these matrices, only $5NM$ operations are needed if $f \neq 0$. Since S_M is the Fourier-sine transform, by using a standard FFT-sine code, the cost for calculating the product of the matrix S_M and a complex vector is $2MlogM$ (real operations). In Step (iv), one solves the system (3.8) for v_{N+1}. A direct method, such as a Gaussian elimination scheme, requires $M^3/3$ complex operations, which is not efficient. Since G is a complex Toeplitz matrix, the product of the coefficient matrix and a complex vector can be performed in terms of *fast Fourier transform* [10], [24] and the cost for calculating the product is only $12MlogM$. If we use the BiCG

TABLE 1
The real operation counts of Algorithm I *for an* $M \times N$ *mesh (p is the number of iterations by BiCG).*

Step	Calculate v with $f \neq 0$	Calculate v_{N+1} with $f = 0$
(i)	$O(M^{1+\sigma})$	O(M)
(ii)	$5NM$	$3NM$
(iii)	$2MNlogM$	0
(iv)	$24pMlogM$	$24pMlogM$
(v)	$O(NMlogM)$	0
Total	$O(NMlogM) + 4pMlogM$	$O(NM) + 24pMlogM$

method or GMRES method for solving the linear systems, the cost of each iteration is $24MlogM$.

In most practical cases of electromagnetic scattering, particularly for radar systems, the fields are source free, i.e., $f(x, y) = 0$. Also, it often suffices to calculate the solution on the interface, i.e., v_{N+1}. In fact, many physical components of interest can be obtained by v_{N+1}. In that case, the solution in the whole computational domain may not be necessary. Hence, the computational procedure can be simplified significantly, and the first part of Steps (iii) and (v) are no longer needed.

The cost (real arithmetic operations) for each step is summarized in Table 1, where p is the number of iterations used for solving the system (3.8) and k is a real number. When $f \neq 0$, the cost of the algorithm is $O(NMlogM)$ if p is not large. More importantly, in the source free case, the cost decreases significantly to $O(M^2)$ for an $M \times M$ mesh if $p \leq M/logM$, which will be illustrated numerically in the next section.

Key to Algorithm I is the iterative solver for the interface system (3.8) with the coefficient matrix

$$\mathcal{A} = I - h_y S_M G S_M + E. \tag{3.11}$$

The efficiency of iterative algorithms for (3.8) depends upon many factors, such as the eigenvalue distribution, the condition numbers of the coefficient matrix, and the regularity of solution.

Consider a unit cavity ($a = b = 1$) and two different media, homogeneous medium $k = k_0$ and layered medium

$$k = \begin{cases} k_0 & -b/3 \leq y < 0, \\ 1.5k_0 & -2b/3 \leq y < -b/3, \\ 2k_0 & -b \leq y < -2b/3. \end{cases} \tag{3.12}$$

We present the eigenvalue distributions of the matrix $\mathcal{A}$ in Figure 2, with respect to some different wave numbers and numbers of mesh points. Observe from Figure 2 that there are some eigenvalues with negative real parts in all cases and the magnitude of the real parts becomes larger as the wave number increases, which may be responsible for the divergence of many classical iterative methods. As a comparison, note that the interface systems arising from Poisson-type equations in some simple domains are symmetric positive definite [8], [9], [11].

In order to solve such an indefinite system, we need an efficient preconditioner. Let $G = G^{re} + \mathrm{i}G^{im}$. Since G is a Toeplitz matrix, we denote by d_{im} the diagonal entries of G^{im}. Then we can rewrite the matrix $\mathcal{A}$ as

$$\mathcal{A} = (I - \mathrm{i}h_y d_{im} I + E) - h_y \left(S_M G S_M - \mathrm{i}d_{im} I\right).$$

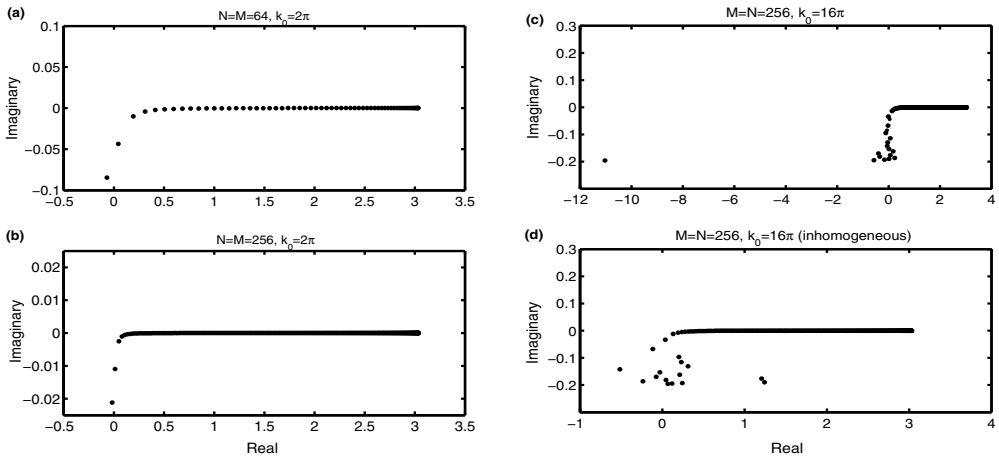

FIG. 2. *The eigenvalue distribution of* $\mathcal{A}$, (a)–(c) *for homogeneous media and* (d) *for the inhomogeneous medium in* (3.12).

TABLE 2
The extremal eigenvalues of the preconditioned matrix $P\mathcal{A}$.

k	N=M	$\min\|\lambda_i\|$	$\max\|\lambda_i\|$	$\max\|\lambda_i\|/\|\min\lambda_i\|$
$k=2\pi$	64	1.505	3.718	2.470
	128	1.487	3.737	2.513
	256	1.478	3.745	2.534
	512	1.473	3.748	2.544
	1024	1.471	3.750	2.550
$k=16\pi$	128	0.8449	7.658	9.064
	256	0.8751	1.453D1	1.661D1
	512	1.003	1.670D1	1.663D1
	1024	1.004	2.164D1	2.154D1
	2048	1.005	2.732D1	2.719D1
k given in (3.12) $k_0=16\pi$	128	0.9871	1.019D1	1.039D1
	256	1.011	4.811	4.758
	512	1.001	6.486	6.482
	1024	1.000	7.332	7.331
	2048	1.000	6.995	6.995

Let

$$P = (I - \mathrm{i}h_y d_{im} I + E)^{-1}$$

be a preconditioner. The interface system (3.8) becomes

$$P\mathcal{A}v_{N+1} = PS_M\hat{g}. \tag{3.13}$$

The extremal eigenvalues and the ratio of the maximal eigenvalue and the minimal eigenvalue of the preconditioned coefficient matrix $P\mathcal{A}$ are given in Table 2. The eigenvalues distributions are presented in Figure 3(a)–(c) for the homogeneous medium $k_0 = 2\pi$ with $N = M = 64$, 256, and 1024, in Figure 3(d) for the homogeneous medium $k = k_0 = 16\pi$, and in Figure 3(e)–(f) for the layered medium defined in (3.12) with $k_0 = 2\pi$ and $k_0 = 16\pi$, respectively.

Several observations are in order:

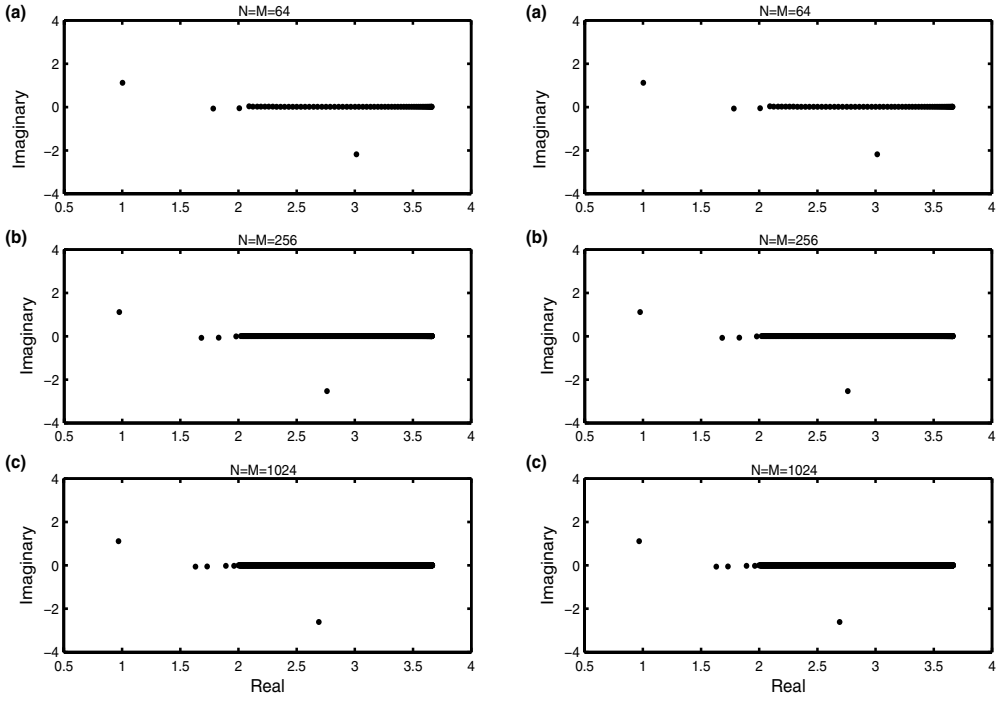

FIG. 3. *The eigenvalue distribution of preconditioned systems with* $\rho = 4.0$, (a)–(c) *homogeneous medium* $k_0 = 2\pi$ *and* (d)–(f) $N = M = 256$.

- In all cases, the real parts of eigenvalues are positive and larger than 0.854. Many iterative algorithms are convergent for such a linear system.
- For the small wave number $k_0 = 2\pi$, the ratio of the maximal eigenvalue and the minimal eigenvalue, which is equivalent to condition number, is almost bounded by a constant 2.55. The eigenvalues distributions are also independent of the number of mesh points. For large wave number $k_0 = 32\pi$, the ratio for the homogeneous medium increases approximately in the order of $M^{0.387}$ and the ratio for the inhomogeneous medium increases slightly as the number of mesh points increases. The minimal eigenvalues are approximately 1 for both homogeneous and inhomogeneous media.
- The ratio of the imaginary part and the real part of eigenvalues is also an important factor for most iterative algorithms. The eigenvalues with a large ratio are called ill-conditioning. For most eigenvalues shown in Table 2 and Figure 3, the imaginary part is smaller than the real part.
  In each case, all eigenvalues are located on a circle of radius about 1.2 to 13, depending on the wavenumber k. All these circles are in the right half-plane and the distance between each circle and the y-axis is larger than 0.85. Certain iterative algorithms are efficient for solving linear systems with this kind of coefficient matrices, such as Krylov subspace methods, and the convergent rate could be independent of the number of mesh points.

3.3. TE case. Rewrite (2.9) of TE case as

$$\begin{aligned} &\frac{\partial^2 u}{\partial x^2}+\frac{\partial^2 u}{\partial y^2}-\frac{k_y}{2k}\frac{\partial u}{\partial y}+k^2 u=k^2 f \qquad (x,y)\in\Omega,\\ &\frac{\partial u}{\partial n}=0 \qquad\qquad \text{on } \partial\Omega\backslash\Gamma,\\ &\frac{\partial u}{\partial n}=\tilde{I}(u)+g \qquad\qquad \text{on } \Gamma. \end{aligned} \tag{3.14}$$

Using the same approximation to the TE equation, we have the discrete system in matrix form

$$\left(A_x^N\otimes I_N+I_M\otimes(A_y^{ND}-D_kB_y^{ND})+I_M\otimes D\right)v+(I_M\otimes a_{N+1})\,v_{N+1}=f, \tag{3.15}$$

where D and a_{N+1} are defined as before, A_x^N denotes the finite difference discrete matrix corresponding to the second-order differential operator with Neumann boundary conditions, and A_y^{ND} and B_y^{ND} denote finite difference matrices corresponding to the second-order and the first-order differential operator with Neumann/Dirichlet boundary conditions, respectively. Thus

$$A_x^N=\frac{1}{h_x^2}\begin{pmatrix} -1 & 1 & & \\ 1 & -2 & 1 & \\ & \ddots & \ddots & \ddots \\ & & 1 & -1 \end{pmatrix} \qquad A_y^{ND}=\frac{1}{h_y^2}\begin{pmatrix} -1 & 1 & & \\ 1 & -2 & 1 & \\ & \ddots & \ddots & \ddots \\ & & 1 & -2 \end{pmatrix}$$

$$B_y^{ND}=\frac{1}{2h_y}\begin{pmatrix} -1 & 1 & & & \\ -1 & 0 & 1 & & \\ & \ddots & \ddots & \ddots & \\ & & -1 & 0 & 1 \\ & & & -1 & 1 \end{pmatrix}$$

and

$$D_k=\frac{1}{2}\begin{pmatrix} \varepsilon'(y_1)/\varepsilon(y_1) & & & \\ & \varepsilon'(y_2)/\varepsilon(y_2) & & \\ & & \ddots & \\ & & & \epsilon'(y_N)/\epsilon(y_N) \end{pmatrix}.$$

A fast algorithm for the TE case can be designed analogously by replacing A_x and A_y in Algorithm I with A_x^N and $A_y^{ND}-D_kB_y^{ND}$.

4. The existence and uniqueness of numerical solution. The existence and uniqueness of the scattering problem (2.1), (2.2) or the equivalent bounded domain problem in (2.8) were proved in [2] and [3]. Here we study the existence and uniqueness of the solution of the discrete system (3.2) with some simple discretization for the nonlocal boundary condition. Let $J_\nu(z)$ and $Y_\nu(z)$ be the Bessel functions. The Hankel function $H_1^1(z)$ is defined by

$$H_1^1(z)=J_1(z)+\mathrm{i}Y_1(z).$$

Since $Y_1(z)$ is hypersingular and $J_1(z)$ is continuous, the nonlocal boundary condition becomes

$$\frac{\partial u}{\partial n} = \frac{\mathrm{i}k_0}{2}\left(\int_0^a \frac{1}{|x-x'|}J_1(k_0|x-x'|)u(x',0)dx' + \mathrm{i}\int_0^a \frac{1}{|x-x'|}Y_1(k_0|x-x'|)u(x',0)dx'\right), \quad x \in (0,a).$$

Let $u(x,0) \approx \sum_{i=1}^{M} \phi_i(x) v_{i,N+1}$, where $\phi_i(x)$, $i = 1, 2, \ldots, M$, denote the piecewise linear basis functions. Then the boundary discrete system can be written by

$$\frac{v_{l,N+1} - v_{l,N}}{h_y} = \sum_{l=1}^{M}(g_{lj}^{re} + \mathrm{i}g_{lj}^{im})v_{j,N+1} + g(x_l), \quad l = 1, 2, \ldots, M,$$

where

$$g_{lj}^{im} = \frac{k_0}{2}\int_0^a \frac{1}{|x-x'|}J_1(k_0|x'-x_l|)\phi_j(x')dx'.$$

By the classical formulation

$$J_1(z) = \frac{z}{\pi}\int_{-1}^{1}(1-t^2)^{1/2}e^{\mathrm{i}zt}\,dt,$$

we have

$$g_{lj}^{im} = \frac{k_0^2}{2\pi}\int_{-1}^{1}(1-t^2)^{1/2}\left(\int_0^a \phi_j(x')e^{\mathrm{i}k_0|x'-x_l|t}\,dx'\right)dt. \tag{4.1}$$

The term g_{lj}^{re} can be calculated by some techniques in [29] since the Hadamard integral is involved.

THEOREM 4.1. *Let $g_{lj} = g_{lj}^{re} + \mathrm{i}g_{lj}^{im}$ and g_{lj}^{im} be defined in* (4.1)*. Then for any real k, the system* (3.2) *attains a unique solution.*

Proof. It suffices to prove that the system (3.2) has only the zero solution when $f = 0$ and $g = 0$. Let v^* denote the conjugate transpose of v. By (3.2)

$$v^*Av + v^*A_{12}v_{N+1} = 0,$$
$$v_{N+1}^*A_{21}v + v_{N+1}^*(I - h_y(G^{re} + \mathrm{i}G^{im}i))v_{N+1} = 0,$$

where $G = G^{re} + \mathrm{i}G^{im}$. Since $A_{21} = -h_y^2A_{12}^T$ and A is real and symmetric,

$$-h_y^2v^*Av + v_{N+1}^*(I - h_yG)v_{N+1} = 0,$$

which leads to

$$v_{N+1}^*G^{im}v_{N+1} = 0. \tag{4.2}$$

It is easy to see that

$$\begin{aligned} g_{lj}^{im} = \frac{k_0^2}{2\pi}\Bigg[&\int_0^1(1-t^2)^{1/2}\int_0^{x_l}\phi_j(x')e^{\mathrm{i}k_0(x'-x_l)t}\,dx'dt \\ &+ \int_0^1(1-t^2)^{1/2}\int_{x_l}^a\phi_j(x')e^{-\mathrm{i}k_0(x'-x_l)t}\,dx'dt \\ &+ \int_{-1}^0(1-t^2)^{1/2}\int_0^{x_l}\phi_j(x')e^{\mathrm{i}k_0(x'-x_l)t}\,dx'dt \\ &+ \int_{-1}^0(1-t^2)^{1/2}\int_{x_l}^a\phi_j(x')e^{-\mathrm{i}k_0(x'-x_l)t}\,dx'dt\Bigg]. \end{aligned}$$

Moreover, by using the change of variables in the last two integrals,

$$\begin{aligned} g_{lj}^{im} &= \frac{k_0^2}{2\pi}\left[\int_0^1 (1-t^2)^{1/2}\int_0^a \phi_j(x')e^{\mathrm{i}k_0(x'-x_l)t}\,dx'dt \right. \\ &\qquad \left. + \int_0^1 (1-t^2)^{1/2}\int_0^a \phi_j(x')e^{-\mathrm{i}k_0(x'-x_l)t}\,dx'dt\right] \\ &= \frac{k_0^2}{\pi}\int_0^1 (1-t^2)^{1/2}\int_0^a \phi_j(x')\cos(k_0(x'-x_l)t)\,dx'dt. \end{aligned}$$

A straightforward calculation gives

$$\int_0^a \phi_j(x')\cos(k_0(x'-x_l)t)\,dx' = \frac{2(1-\cos(k_0th_x))\cos((j-l)k_0th_x)}{t^2k_0^2h_x}.$$

Hence

$$g_{lj}^{im} = \frac{2}{\pi h_x}\int_0^1 \eta(t)\cos((j-l)k_0th_x)\,dt, \tag{4.3}$$

where $\eta(t) = (1-t^2)^{1/2}(1-\cos(k_0th_x))/t^2$. It follows that G^{im} is a symmetric Toeplitz matrix and furthermore

$$\begin{aligned} v_{N+1}^* G^{im} v_{N+1} &= \sum_{l=1}^M\sum_{j=1}^M g_{lj}^{im} v_{l,N+1}^* v_{j,N+1} \\ &= \frac{2}{\pi h_x}\sum_{l=1}^M\sum_{j=1}^M \int_0^1 \eta(t)\cos((j-l)k_0th_x)v_{l,N+1}^* v_{j,N+1}\,dt \\ &= \frac{1}{\pi h_x}\int_0^1 \eta(t)\sum_{l=1}^M\sum_{j=1}^M \left(e^{\mathrm{i}k_0(j-l)th_x} + e^{-\mathrm{i}k_0(j-l)th_x}\right) v_{l,N+1}^* v_{j,N+1}\,dt \\ &= \frac{1}{\pi h_x}\int_0^1 \eta(t)\left(\left|\sum_{j=1}^M e^{\mathrm{i}k_0jth_x}v_{j,N+1}\right|^2 + \left|\sum_{l=1}^M e^{-\mathrm{i}k_0lth_x}v_{l,N+1}\right|^2\right)\,dt. \end{aligned}$$

By (4.2), we have

$$\sum_{j=1}^M e^{\mathrm{i}k_0jth_x}v_{j,N+1} = 0\,, \quad \sum_{j=1}^M e^{-\mathrm{i}k_0jth_x}v_{j,N+1} = 0 \quad \text{for } 0<t<1 \tag{4.4}$$

which leads to $v_{j,N+1} = 0$, $j = 1, 2, \ldots, M$. From the second system in (3.2), $v_{j,N} = 0$ and we deduce further that $v_{ij} = 0$ from the first system in (3.2). The proof is complete. ∎

In practice, one may calculate g_{lj}^{im} numerically. A general quadrature form can be given by

$$g_{lj}^{im} \approx \frac{2}{\pi h_x}\sum_{m=1}^{M'} \omega_m\eta(t_m)\cos((j-l)k_0t_mh_x), \tag{4.5}$$

where w_m denotes the weight, and an alternative approximation is given by

$$g_{lj}^{im} \approx \frac{2}{\pi h_x}\int_0^1 \eta_h(t)\cos((j-l)k_0th_x)\,dt, \tag{4.6}$$

where $\eta_h(t)$ denotes a general approximation to $\eta(t)$ satisfying $\eta_h(t) > 0$ for $t \in (0,1)$. The following corollary can be obtained immediately.

COROLLARY 4.2. *Let* $g_{lj} = g_{lj}^{re} + \mathrm{i}g_{lj}^{im}$ *and* g_{lj}^{im} *be given by* (4.5) *with* $M' \geq M/2$ *or in* (4.6). *Then for any real* k, *the system* (3.2) *has a unique solution.*

5. Numerical experiments. In this section, computational results are reported for two examples to test our algorithm. Our focus is on the efficiency of our algorithm to solve the discrete linear systems. Once again, error analysis of the discrete method and other high order methods remains open. Throughout, the computation is performed on a Blade 1000 Sun-workstation in double precision. The BiCG method given in [10] is applied to solve the system (3.13).

Example 5.1. Consider a plane wave scattering from a rectangular groove with 1 meter wide and 0.25 meter deep at normal incidence ($a = 1.0$ and $b = 0.25$). Two different cases are considered: the groove filled with a homogeneous medium $k = k_0$ and the groove filled with some inhomogeneous medium defined in (3.12). The former has been a standard test problem [23], [41]. Numerical results are obtained by using our algorithm with 128 nodal points at each coordinate direction for the homogeneous case $k = k_0 = 2\pi$. The magnitude and phase of the field are given in Figure 4(a)–(b), compared with the experimental results in [11]. The physical parameter of interest is the RCS, which is defined by

$$\sigma = \frac{4}{k_0}|P(\phi)|^2,$$

where ϕ is the observation angle and P is the far-field coefficient given by

$$P(\phi) = \frac{k}{2}\sin\phi \int_\Gamma u e^{\mathrm{i}kx\cos\phi} dx.$$

The backscatter RCS(b), compared with experimental results in [23], is given in Figure 4(c).

Next, we consider problems with the high wave number $k_0 = 32\pi$ for both the homogeneous medium and the layered medium defined by (3.12). We present in Figure 4(d)–(f) the magnitudes of the fields on Γ, where $M = N = 1024$ and $\theta = 0$. Since no analytic solution is available, numerical solutions with $N = M = 2048$ are also calculated to confirm the convergence.

We use the BiCG method in Step (iv) to solve the linear system (3.13). As usual, the iteration stops with the absolute residual

$$e_R = \left(\frac{1}{M} \sum_{i=1}^{M} \left(\hat{g}_i - \sum_{j=1}^{M} a_{ij} v_{j,N+1}^p \right)^2 \right)^{1/2} \leq \delta,$$

where v^p is the numerical solution at the pth iteration and $P\mathcal{A} = (a_{ij})$. The CPU time for each step, the total CPU time, and the number of iterations in Step (iv) by the BiCG method are shown in Table 3 until $N = M = 4096$, where $\delta = h_x h_y/5$. The CPU time in Step (i) is proportional to M, the number of mesh points, since we have used an approximation independent of h_x, while the CPU time in Step (ii) is proportional to M^2.

Clearly, the number of iterations (p) in Step (iv) is almost independent of the number of mesh points and increases as the wavenumber k increases (approximately

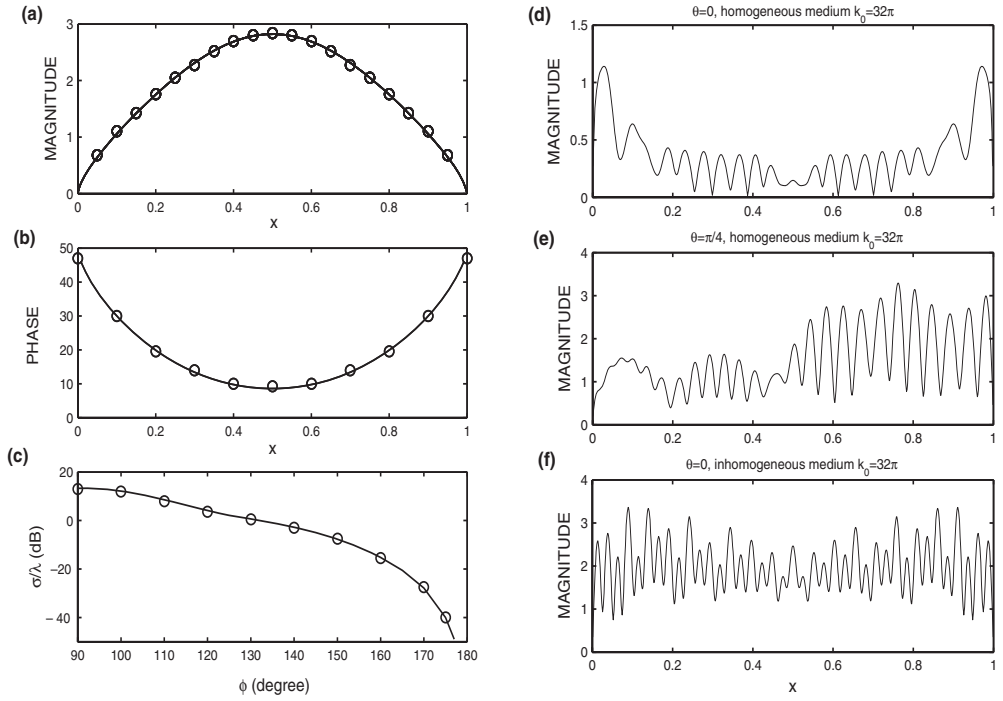

FIG. 4. *Aperture electric field and backscatter RCS.* (a)–(c) *normal incidence* ($\theta = 0$) *and homogeneous medium* $k_0 = 2\pi$ *and* (d)–(f) $k_0 = 32\pi$ *(Example* 5.1*).*

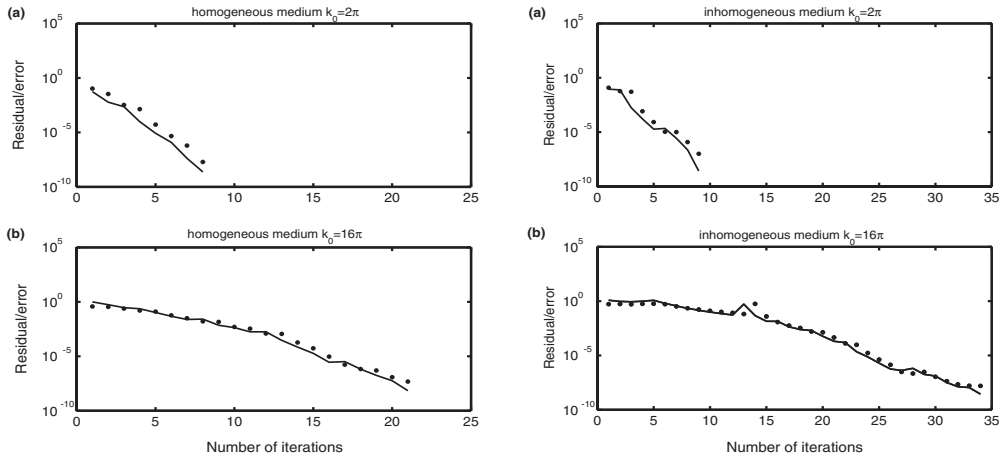

FIG. 5. *The hysteresis of convergence of the BiCG method for solving* (3.13) *with* $N = M = 512$*, where the solid line denotes the residual* e_R *and dashed line the error* e_G*.* (a) $k = 2\pi$*,* (b) $k = 16\pi$*, and* (c) k *is defined in* (3.12) *with* $k_0 = 16\pi$ *and* $\rho = 1$ *(Example* 5.1*).*

with $p = 4 + k/(2\pi)$). The results are in good agreement with our analysis. We present the convergence hysteresis of the BiCG method in Figure 5, where the solid

TABLE 3
CPU time (sec.) and the number of iterations for Example 5.1 *with* $\delta = h_x h_y/5$.

k	No. of unknowns (MN)	CPU (Step (i))	CPU (Step (ii))	CPU (No. of iteration) (Step (iv))	Total CPU
$k = 2\pi$	256^2	0.1181	0.0148	0.0405 (4 iterations)	0.1804
	512^2	0.2372	0.0594	0.1012 (4 iterations)	0.4013
	1024^2	0.4783	0.2375	0.2289 (4 iterations)	0.9467
	2048^2	0.9551	0.9873	0.4832 (4 iterations)	2.412
$k = 4\pi$	256^2	0.1502	0.0150	0.0502 (5 iterations)	0.1804
	512^2	0.3145	0.0598	0.1509 (6 iterations)	0.5268
	1024^2	0.6350	0.2376	0.3424 (6 iterations)	1.230
	2048^2	1.303	0.9876	0.7212 (6 iterations)	3.110
$k = 8\pi$	256^2	0.1906	0.0150	0.0799 (8 iterations)	0.2912
	512^2	0.3903	0.0597	0.2005 (8 iterations)	0.6587
	1024^2	0.8043	0.2379	0.5140 (9 iterations)	1.623
	2048^2	1.723	0.9882	1.073 (9 iterations)	3.867
$k = 16\pi$	256^2	0.2420	0.0152	0.1211 (12 iterations)	0.4122
	512^2	0.4853	0.0598	0.2776 (13 iterations)	0.8322
	1024^2	0.9770	0.2385	0.6164 (13 iterations)	1.867
	2048^2	1.972	0.9894	1.478 (14 iterations)	4.431
	4096^2	3.916	4.141	3.267 (15 iterations)	11.44
k given in (3.12) ($k_0 = 8\pi$)	256^2	0.2431	0.0153	0.1206 (12 iterations)	0.3827
	512^2	0.4889	0.0602	0.2636 (12 iterations)	0.8213
	1024^2	0.9856	0.2388	0.5812 (12 iterations)	1.832
	2048^2	1.974	0.9937	1.332 (12 iterations)	4.398
	4096^2	3.947	4.141	3.103 (13 iterations)	11.24

line represents the residual defined above and the dashed line denotes the L_2 error

$$e_G = \left(\frac{1}{M} \sum_{i=1}^{M} (v_{i,N+1}^p - v_{i,N+1}^G)^2 \right)^{1/2}.$$

Here $v_{i,N+1}^G$ is the solution obtained by the Gaussian elimination.

Our numerical experiments illustrate that the computational complexity for the solution v_{N+1} is $O(M^2)$ for an $M \times M$ mesh.

Example 5.2. We consider an artificial example defined by (2.8) with a large cavity $a = b = 1$ to test the accuracy of approximation. The $f(x, y)$ and $g(x)$ are chosen such that the exact solution is

$$u(x, y) = e^{xy} \left(\sin \frac{k_0 x}{2} \right) \sin \left(\frac{k_0}{2} + \frac{\pi}{4} \right) y.$$

The error measures in the L_2 norm and the L_∞ norm in the domain Ω are defined by

$$e_2(\Omega) = \left(\tfrac{1}{(N+1)M} \textstyle\sum_{i,j=1}^{M,N+1} (u_{ij}^h - u(x_i, y_j))^2 \right)^{1/2},$$
$$e_M(\Omega) = \max_{i,j} |u_{ij}^h - u(x_i, y_j)|,$$

where u_{ij}^h denotes the numerical solution at the point (x_i, y_j). Since the solution at the top line of cavity (interface) is more important, we also define the following error

TABLE 4
Error results for Example 5.2.

k	No. of unknowns (MN)	$e_M(\partial\Omega)$	$e_2(\partial\Omega)$	$e_M(\Omega)$	$e_2(\Omega)$
$k = k_0 = 2\pi$	64^2	8.384D-3	6.226D-2	1.170D-2	6.123D-3
	128^2	4.334D-3	3.197D-3	5.986D-3	3.149D-3
	256^2	2.203D-3	1.620D-3	3.032D-3	1.597D-3
	512^2	1.110D-3	8.152D-4	1.533D-3	8.040D-4
	1024^2	5.575D-4	4.089D-4	7.707D-4	4.024D-4
$k = k_0 = 32\pi$	64^2	6.601D-2	2.989D-2	2.873D-1	8.342D-2
	128^2	7.585D-2	4.327D-2	9.404D-2	3.039D-2
	256^2	3.387D-2	1.630D-2	7.249D-2	3.120D-2
	512^2	2.215D-2	1.165D-2	2.935D-2	1.250D-2
	1024^2	1.110D-2	5.945D-3	1.409D-2	5.979D-3
k given in (3.13) $k_0 = 32\pi$	64^2	1.544D-1	7.433D-2	1.544D-1	1.577D-2
	128^2	6.278D-2	3.684D-2	7.042D-2	2.669D-2
	256^2	3.453D-2	1.730D-2	5.490D-2	2.501D-2
	512^2	1.790D-2	9.243D-3	2.164D-2	7.358D-3
	1024^2	1.036D-2	6.008D-3	1.127D-2	4.796D-3

measures on Γ,

$$e_2(\Gamma) = \left(\tfrac{1}{M}\sum_i^M (u^h_{i,N+1} - u(x_i,0))^2\right)^{1/2},$$
$$e_M(\Gamma) = \max_{i,j} |u^h_{i,N+1} - u(x_i,0)|.$$

We analyze the errors in Table 4 with different wave numbers and different numbers of mesh points. It is evident that for the small wave number $k = k_0 = 2\pi$, the error is always in the order of $O(h)$. Since we use a first-order scheme for $\frac{\partial u}{\partial n}$, this is in good agreement with theoretical analysis. For the large wave number $k = k_0 = 32\pi$, however, the order pattern of errors is not clear for small M, $M = 64, 128$. By increasing M, we can still see the first-order accuracy in the numerical results. However, the errors for problems with large wave numbers are much larger than those for small wave numbers. This confirms previous theoretical analysis and the claim that the best error estimate is achieved only when the condition "$k^2h = constant$" is satisfied. Nevertheless, since the computational complexity of our algorithm is $O(M^2)$ for an $M \times M$ mesh and the memory requirement is $O(M)$ for calculating the RCS, our algorithm can be applied to solve model problems with very large numbers of mesh points.

6. Concluding remarks. A new fast algorithm is presented for solving electromagnetic scattering from a rectangular open (layered) cavity. The algorithm is designed to use the FFT in the layered direction and Gaussian elimination along the inhomogeneous direction to solve the discrete linear systems.

Based on our numerical experiments, the proposed complex preconditioner is efficient. However, theoretical analysis remains open. The problem is challenging mainly due to the complicated transparent boundary condition and the indefinite Dirichlet Helmholtz operator.

Our algorithm has the advantages of being simple in structures and easy to implement, in addition to its capability of handling large cavities or high wave numbers. It is also flexible enough to be incorporated with many types of discretization of the underlying model PDEs. The fast algorithm provides an alternative to the current

efforts of designing sophisticated basis functions for solving Helmholtz equations with high wave numbers.

We point out two important future directions along the line of our present work. The first is to solve the scattering from three-dimensional large cavities. Our algorithm may be extended to provide a fast solver for layered three-dimensional cavities and a preconditioner for two-dimensional problems with more general medium distribution. The algorithm for solving the resulting discrete systems may be designed again by a combination of the FFT and a Gaussian elimination scheme. Another important project is to apply our fast algorithm to the optimal design problems. An example is to design the shape and composition of a layered cavity to minimize the RCS. Computationally, the design problem can be challenging because of the need of solving the scattering problem repeatedly. The fast algorithm presented here certainly would provide the essential tool for the design problems. In addition, it is possible to extend existing preconditioning techniques for Toeplitz systems; e.g., see [10] and [24], to the interface system (3.8).

Acknowledgments. The authors would like to thank Professors Su, Chaowei, and Wu Ji-ming for providing a BiCG code and a code for the discretization of the nonlocal boundary conditions. We also thank Professor Howard Elman and the referee for useful suggestions and for informing us of several related references.

REFERENCES

[1] L. Abrahamsson and H. Kreiss, *Numerical solution of the coupled mode equations in duct acoustics*, J. Comput. Phys., 111 (1994), pp. 1–14.

[2] H. Ammari, G. Bao, and A. W. Wood, *An integral equation method for the electromagnetic scattering from cavities*, Math. Methods Appl. Sci., 23 (2000), pp. 1057–1072.

[3] H. Ammari, G. Bao, and A. W. Wood, *Analysis of the electromagnetic scattering from a cavity*, Japan J. Indust. Appl. Math., 19 (2002), pp. 301–310.

[4] A. K. Aziz, R. B. Kellogg, and A. B. Stephen, *A two point boundary value problem with a rapidly oscillating solution*, Numer. Math., 53 (1988), pp. 107–121.

[5] I. Babuska and S. A. Sauter, *Is the pollution effect of the FEM avoidable for the Helmholtz equation considering high wave numbers?* SIAM J. Numer. Anal., 34 (1997), pp. 2392–2423.

[6] I. Babuska, F. Ihlenburg, E. T. Paik, and S. A. Sauter, *A generalized finite element method for solving the Helmholtz equation in two dimensions with minimal pollution*, Comput. Methods Appl. Mech. Engrg., 128 (1995), pp. 325–359.

[7] R. E. Bank, *Efficient algorithms for solving tensor product finite element equations*, Numer. Math., 31 (1978/79), pp. 49–61.

[8] P. E. Bjorstad and O. B. Widlund, *Iterative methods for the solution of elliptic problems on regions partitioned into substructures*, SIAM J. Numer. Anal., 23 (1986), pp. 1097–1120.

[9] B. L. Buzbee, F. W. Dorr, J. A. George, and G. H. Golub, *The direct solution of the discrete Poisson equation on irregular regions*, SIAM J. Numer. Anal., 8 (1971), pp. 722–736.

[10] R. H. Chan and M. K. Ng, *Conjugate gradient methods for Toeplitz systems*, SIAM Rev., 38 (1996), pp. 427–482.

[11] T. F. Chan and T. Y. Hou, *Eigendecomposition of domain decomposition interface operators for constant coefficient elliptic problems*, SIAM J. Sci. Statist. Comput., 12 (1991), pp. 1471–1479.

[12] H. Elman and D. P. O'Leary, *Efficient iterative solution of the three-dimensional Helmholtz equation*, J. Comput. Phys., 142 (1998), pp. 163–181.

[13] H. Elman and D. P. O'Leary, *Eigenanalysis of some preconditioned Helmholtz problems*, Numer. Math., 83 (1999), pp. 231–257.

[14] H. Elman, O. G. Ernst, and D. P. O'Leary, *A multigrid method enhanced by Krylov subspace iteration for discrete Helmholtz equations*, SIAM J. Sci. Comput., 23 (2001), pp. 1291–1315.

[15] B. Engquist and A. Majda, *Absorbing boundary conditions for the numerical simulation of waves*, Math. Comp., 31 (1977), pp. 629–651.

[16] O. G. Ernst, *Fast Numerical Solution of Exterior Helmholtz Problems with Radiation Boundary Condition by Imbedding*, Ph.D. thesis, Stanford University, Stanford, CA, 1994.
[17] O. G. Ernst, *A finite-element capacitance matrix method for exterior Helmholtz problems*, Numer. Math., 75 (1996), pp. 175–204.
[18] O. G. Ernst and G. H. Golub, *A domain decomposition approach to solving the Helmholtz equation with radiation boundary condition*, Contemp. Math, 157 (1994), pp. 177–192.
[19] G. Fix and S. P. Marin, *Variational methods for underwater acoustic problems*, J. Comput. Phys., 28 (1978), pp. 253–270.
[20] D. Givoli, *Numerical Methods for Problems in Infinite Domains*, Stud. Appl. Mech. 33, Elsevier, Amsterdam, 1992.
[21] E. Heikkola, T. Rossi, and J. Toivanen, *A parallel fictitious domain method for the three-dimensional Helmholtz equation*, SIAM J. Sci. Comput., 24 (2003), pp. 1567–1588.
[22] D. A. Jacobs, *A generalization of the conjugate-gradient method to solve complex systems*, IMA J. Numer. Anal., 6 (1986), pp. 447–452.
[23] J. Jin, *The Finite Element Method in Electromagnetics*, John Wiley & Sons, New York, 1993.
[24] X. Q. Jin, *Developments and Applications of Block Toeplitz Iterative Solvers*, Science Press & Kluwer Academic Publishers, Beijing/Dordrecht, The Netherlands, 2002.
[25] J. B. Keller and D. Givoli, *Exact nonreflecting boundary conditions*, J. Comput. Phys., 82 (1989), pp. 172–192.
[26] S. Kim, *Domain decomposition iterative procedures for solving scalar waves in the frequency domain*, Numer. Math., 79 (1998), pp. 231–259.
[27] J. Liu and J. M. Jin, *A special higher-order finite-element method for scattering by deep cavity*, IEEE Trans. Antennas Propag., 48 (2000), pp. 694–703.
[28] R. C. MacCamy and S. P. Marin, *A finite element method for exterior interface problems*, Internat. J. Math. Math. Sci., 3 (1980), pp. 311–350.
[29] P. A. Martin, F. J. Rizzo, and T. A. Cruse, *Smoothness-relaxation strategies for singular and hypersingular integral equations*, Internat. J. Numer. Methods Engrg., 42 (1998), pp. 885–906.
[30] D. P. O'Leary and O. Widlund, *Capacitance matrix methods for the Helmholtz equation on general three-dimensional regions*, Math. Comp., 33 (1979), pp. 849–879.
[31] K. Otto and E. Larsson, *Iterative solution of the Helmholtz equation by a second-order method*, SIAM J. Matrix Anal. Appl., 21 (1999), pp. 209–229.
[32] A. F. Peterson, *Analysis of heterogeneous electromagnetic scatterers: Research progress of the past decades*, Proc. IEEE, 79 (1991), pp. 1431–1441.
[33] W. Proskurowski, *Capacitance matrix methods—a brief survey*, in Elliptic Problem Solvers, Academic Press, New York, 1981, pp. 391–398.
[34] D. C. Ross, J. L. Volakis, and H. T. Anastassiu, *Hybrid finite element-modal analysis of jet engine inlet scattering*, IEEE Trans. Antennas Propag., 43 (1995), pp. 277–285.
[35] P. R. Rousseau and R. J. Burkholder, *A hybrid approach for calculating the scattering from obstacles within large, open cavities*, IEEE Trans. Antennas Propag., 43 (1995), pp. 1068–1075.
[36] W. Sun, *Fast algorithms for high-order spline collocation systems*, Numer. Math., 81 (1998), pp. 143–160.
[37] W. Sun and J. Wu, *Newton-Cotes formulas for numerical evaluation of certain hypersingular integrals*, Computing, to appear.
[38] W. Sun and N. G. Zamani, *A fast algorithm for solving the tensor product collocation equations*, J. Franklin Inst., 326 (1989), pp. 295–307.
[39] P. N. Swarztrauber, *The methods of cyclic reduction, Fourier analysis, and the FACR algorithm for the discrete solution of Poisson's equation on a rectangle*, SIAM Rev., 19 (1977), pp. 490–501.
[40] P. N. Swarztrauber, *Fast Poisson solvers*, in Studies in Numerical Analysis, G. H. Golub, ed., MAA Stud. Math., 24, Math. Assoc. America, Washington, D.C., 1984, pp. 319–370.
[41] T. Van and A. W. Wood, *A time-domain finite element method for Helmholtz equations*, J. Comput Phys., 183 (2002), pp. 486–507.
[42] Z. Xiang and T. T. Chia, *A hybrid BEM/WTM approach for analysis of the EM scattering from large open-ended cavities*, IEEE Trans. Antennas Propag., 49 (2001), pp. 165–173.